J. Biochem. 2010;148(3):309–318 doi:10.1093/jb/mvq067

JB THE JOURNAL OF BIOCHEMISTRY

Disulphide cross-linking between the stator and the bearing components in the bacterial flagellar motor

Received April 28, 2010; accepted June 17, 2010; published online June 23, 2010

Yohei Hizukuri*, Seiji Kojima and Michio Homma†

Division of Biological Science, Graduate School of Science, Nagoya University, Furo-Cho, Chikusa-Ku, Nagoya 464-8602, Japan

*Present address: Institute for Virus Research, Kyoto University, 53 Kawahara-Cho, Shogoin, Sakyo-Ku, Kyoto 606-8507, Japan

†Michio Homma, Division of Biological Science, Graduate School of Science, Nagoya University, Furo-Cho, Chikusa-Ku, Nagoya 464-8602, Japan, Tel: +81-52-789-2991, Fax: +81-52-789-3001, email: g44416a@cc.nagoya-u.ac.jp

The flagellar motor is composed of the stator and the rotor, and the interaction between the stator and the rotor at the cytoplasmic region is believed to produce mechanical force for the rotation of flagella. The periplasmic region of the stator has been proposed to play an important role in assembly around and incorporation into the motor. In this study, we provide evidence suggesting that the periplasmic region of the stator component MotB interacts with the P-ring component FlgI, which functions as a bearing for the rotor along with the L-ring protein FlgH, from a site-directed disulphide cross-linking approach. First, we prepared four FlgI and three MotB cysteine-substituted mutant proteins and co-expressed them in various combinations in *Escherichia coli*. We detected cross-linked combinations of FlgI G11C and MotB S248C when treated with the oxidant Cu-phenanthroline or bismaleimide cross-linkers. Furthermore, we performed Cys-scanning mutagenesis around these two residues and found additional combinations of cross-linked residues. Treatment with a protonophore CCCP significantly reduced the cross-linking efficiency between FlgI and MotB in flagellated cells, but not in non-flagellated cells. These results suggest a direct contact between MotB and FlgI upon assembly of the stator into a motor.

Keywords: bacterial flagella/disulphide bond/*Escherichia coli*/P ring/stator.

Abbreviations: BMB, 1,4-bis(maleimido)butane; BMH, bis(maleimido)hexane; BMOE, bis(maleimido) ethane; CCCP, carbonyl cyanide *m*-chlorophenylhydrazone; DMSO, demethylsulfoxide; DPDPB, 1,4-di-[3′-(2′-pyridyldithio)propionamido]butane; DTNB, 5,5′-dithiobis-2-nitrobenzoic acid; PG, peptidoglycan; PGB, peptidoglycan binding; TM, transmembrane; TMEA, tris-[2-maleimidoethyl]amine.

The bacterial flagellum is an organelle for locomotion that rotates like a screw. Each flagellum consists of three substructures: a long helical filament extending from the cell body, a motor that is embedded in the cell membrane and a flexible hook that connects these two structures. Flagellar rotation is generated by the motor, which is composed of a basal body (a rotor) and a stator. In Gram-negative bacteria such as *Escherichia coli* and *Salmonella enterica* serovar Typhimurium, the flagellar basal body consists of several ring structures surrounding a rod that penetrates the cell envelope (*1*). The L, P and MS rings are located in the outer membrane, the periplasm or the peptidoglycan (PG) layer and the cytoplasmic membrane, respectively, whereas the C ring lies on the cytoplasmic side of the MS ring (Fig. 7B). On the other hand, the stator is a membrane protein complex that conducts protons to generate torque (*2*–*5*). The driving force for rotation of the flagellar motor is generated by converting the electrochemical proton gradient into mechanical force.

The P ring forms a stiff cylindrical structure along with the L ring (*6*). The L–P ring complex is believed to hold the central rod as a bushing; thus it is thought to be a non-rotating component. The P ring consists of 26 copies of a single protein, FlgI (*7*, *8*), which is expressed as a precursor form with a cleavable N-terminal 19 amino acid leader sequence. FlgI is exported to the periplasmic space via the Sec apparatus (*9*) and assembles into the P ring surrounding the rod in the presence of FlgA which acts as a periplasmic chaperon (*10*, *11*). The mature FlgI forms an intramolecular disulphide bond for stabilization of the protein (*12*, *13*). We have previously performed systematic Cys mutagenesis on the FlgI protein, and identified the residues that are important for protein stability and cell motility, and the residues that are exposed to solvent on the surface of the protein (*14*). From this analysis we have proposed that the highly conserved N-terminal region of FlgI is important in maintenance of the structure of FlgI or formation of an interface with other flagellar proteins or with itself.

The stator is composed of two membrane proteins in *E. coli*, MotA and MotB. MotA has four transmembrane (TM) regions and a large cytoplasmic loop (*15*), whereas MotB has a single N-terminal TM region and a large C-terminal periplasmic region (*16*). Four MotA and two MotB proteins constitute one stator complex (*17*–*20*), and at least 11 stators are thought to surround the basal body (*21*). The cytoplasmic loop of MotA is widely believed to electrostatically interact with FliG, resulting in torque generation (*22*). The C-terminal periplasmic region of MotB has a consensus peptidoglycan-binding (PGB) motif, so MotB is believed to associate with the PG layer via this region to stabilize the stator around the basal body (*23*, *24*). Recently crystal structures of the C-terminal

periplasmic region of MotB from *Helicobacter pylori* (*25*) and *S. enterica* serovar Typhimurium (*26*) have been reported and turned out to be very similar in domain structure to Pal, which also has the PGB motif and has been demonstrated to bind to the PG layer (*27–30*). Consistent with this similarity, we have reported that a chimeric protein that has the N-terminal TM region of MotB and the C-terminal periplasmic region of Pal of *E. coli* is partially functional if it has only a single mutation at its junction site (*31*). FRAP analysis of a single motor observation revealed that the stator complexes incorporated into the basal body are exchanged frequently with the ones present in the membrane pool around the motor (*32*). Furthermore, in *Vibrio* (*33*) and *Shewanella* (*34*) species, the stator association and dissociation, or their exchange, are dependent on their coupling ions. These recent findings revealed that the movement of the stator complex seems more dynamic than we previously thought. This view raised some questions: how and where does the stator recognize and target to the basal body when the membrane-pooled stator complex assembles around the basal body?

Deletion analysis of the C-terminal region of PomB (*35*), which is a *Vibrio* homolog of MotB, and fluorescent observation of the GFP-fused C-terminal-truncated PomB (*36*) have revealed that the C-terminal PGB region is essential for assembly of the stator complex around the flagellar basal body. Moreover, in *Salmonella* species, since over-expression of the C-terminal periplasmic domain of MotB strongly inhibits motility of wild-type cells when it is exported into the periplasm, we have proposed that the C-terminal periplasmic domain of MotB plays an important role in proper assembly of the stator complex into a motor (*37*). In *Vibrio* species, the T ring, which is composed of MotX and MotY, is located on the periplasmic side of the P ring. In the absence of MotX and/or MotY, the stator complexes cannot be localized to the flagellated cell pole where the basal body or the rotor is located (*38*). This suggests that the T ring interacts with the stator complex via the interaction between MotX and PomB (*39*). From this evidence the T ring is proposed to play an essential role in the incorporation and stabilization of the stator in *Vibrio*. In contrast, bacteria such as *E. coli* and *Salmonella* do not possess MotX and MotY, raising the possibility that the P ring may have a similar role to the T ring for incorporation of the stator into the motor.

To test whether the P ring and the stator directly contact with each other in a functional motor, we examined cross-linking experiment between the component proteins, FlgI and MotB. As described above, we have systematically generated a series of Cys-substituted mutants of FlgI, and recently we did a similar analysis for the periplasmic region of MotB (*14*, *31*). Therefore, we co-expressed these mutant proteins in various combinations, and examined the formation of disulphide cross-links between them. We detected disulphide cross-bridges in some combinations and further analysed these cross-linked products.

Materials and Methods

Bacterial strains, growth conditions and media

The *E. coli* strains used in this work are listed in Table I. *E. coli* cells were cultured at 37°C or at 30°C in LB medium (1% Bacto tryptone, 0.5% yeast extract and 0.5% NaCl) or in TG medium [1% Bacto tryptone, 0.5% NaCl and 0.5% (w/v) glycerol]. When necessary, ampicillin and kanamycin were added to a final concentration of 50 μg/ml. Expression from the *araBAD* promoter was induced by adding 0.04% L-arabinose to cultures.

Construction of plasmids

To construct Cys-substituted FlgI or MotB variants, site-directed mutagenesis using *Pfu Ultra* High-Fidelity DNA Polymerase (Stratagene) was performed as described previously (*14*).

Detection of proteins

Immunoblotting analysis was performed using anti-*E. coli* FlgI antibodies (FlgI346, *13*) or anti-*E. coli* MotB peptide antibodies (MotB2, *31*), as described previously.

Motility assays

Swarming ability was assayed as follows. Two microlitres of overnight cultures (grown on LB medium at 37°C) were dropped on a soft agar T broth plate (1% Bacto tryptone, 0.5% NaCl and 0.27% Bacto agar) containing 50 μg/ml ampicillin and kanamycin. To induce protein production, 0.04% L-arabinose was included in the plate. The plates were incubated at 30°C for indicated time.

Disulphide cross-linking by Cu-phenanthroline

In vivo disulphide cross-linking was performed in the presence of Cu(II)(1,10-phenanthroline)$_3$ (referred to as Cu-phenanthroline in this article) by a previously described method (*31*) with slight modifications. Sixty micro molar Cu-phenanthroline solution [60 mM $Cu(II)SO_4$-$5H_2O$, 200 mM 1,10-phenanthroline monohydrate (nakalai tesque), 50 mM $NaHPO_4$ (pH 7.8)] was stored at −20°C in the dark. Cells in exponential growth phase ($OD_{660} = 1.0$) from 0.8 ml of TG medium containing 50 μg/ml ampicillin and kanamycin and 0.04% L-arabinose at 30°C were harvested by centrifugation, and suspended in 1 ml of Wash buffer (10 mM potassium phosphate buffer, pH 7.0, containing 0.1 mM EDTA-K). Cells were divided into two aliquots, then centrifuged and resuspended in 100 μl of MLM buffer (Wash buffer containing 10 mM DL-lactate/KOH and 0.1 mM L-methionine). To each sample was added 100 μl of MLM buffer with or without 2 mM Cu-phenanthroline (final concentration of 1 mM) and incubated at room temperature for 30 min. in the dark. To stop the reaction, 40 μl of 6 × Stop solution (210 mM Tris-HCl, pH 7.0, 15 mM EDTA-Na, pH 7.0, 15 mM *N*-ethylmaleimide) was added. Each sample was centrifuged again and washed with 500 μl of Wash buffer. Washed samples were centrifuged, resuspended in 20 μl of SDS loading buffer without 2-mercaptoethanol and boiled at 100°C for 5 min. Samples were separated by SDS-PAGE and analysed by immunoblotting.

Table I. *Escherichia coli* strains and plasmids.

Strain or plasmid	Genotype or description	References or source
Strains		
RP437	F$^-$ *thi thr leu his met eda rpsL*, wild-type for chemotaxis	(*46*)
YZ12-1	RP437 Δ*flgI* Δ*motAB*::*cat*	(*14*)
RP3098	Δ(*flhD-flhA*)*4*	(*47*)
Plasmids		
pBAD24	P_{BAD} *araC* Amp^r	(*48*)
pSU38	P_{lac} *lacZ*α Km^r	(*49*)
pJN726	pBAD24 *Ec motAB*	(*14*)
pYZ301	pSU38 *Ec flgI*	(*14*)

Amp^r, ampicillin resistant; Km^r, kanamycin resistant; P_{BAD}, *araBAD* promoter; P_{lac}, *lac* promoter; *Ec*, *Escherichia coli*.

Disulphide cross-linking by bismaleimide cross-linkers

In vivo disulphide cross-linking using bis(maleimido)hexane (BMH), 1,4-bis(maleimido)butane (BMB) or bis(maleimido)ethane (BMOE) (all cross-linkers from Pierce Biotechnology) was performed as described below. Each cross-linker was stored as a 20 mM stock solution in demethylsulfoxide (DMSO) at −20°C in the dark. Cells were grown to exponential growth phase ($OD_{660} = 1.0$) in TG medium containing appropriate antibiotics and 0.04% L-arabinose at 30°C and were harvested from 1.6 ml cultures by centrifugation at 25°C and suspended in 1 ml of Wash buffer. Cells were centrifuged again and resuspended in 400 µl of MLM Buffer. Cells were divided into four aliquots and 100 µl of MLM Buffer containing 0, 4, 40 or 400 µM of each cross-linker (final concentrations were 0, 2, 20 or 200 µM, respectively) was added, and samples were incubated at room temperature for 1 h in the dark. After incubation each sample was centrifuged and washed with 500 µl of Wash Buffer. If necessary, free swimming of the cells was observed using dark-field microscopy. Each sample was centrifuged, resuspended in 20 µl of SDS loading buffer containing 2-mercaptoethanol and boiled at 100°C for 5 min. Samples were separated by SDS–PAGE and analysed by immunoblotting.

CCCP treatment

Treatment with the protonophore, carbonyl cyanide *m*-chlorophenylhydrazone (CCCP) and subsequent cross-linker treatment were performed as follows. CCCP was stored as a 20 mM stock solution in DMSO at −20°C in the dark. Cells in exponential growth phase ($OD_{660} = 1.0$) from 0.8 ml of TG medium containing appropriate antibiotics and 0.04% L-arabinose (grown at 30°C) were harvested by centrifugation at 25°C and suspended in 1 ml of Wash buffer. Cells were centrifuged again and resuspended in 200 µl of MLM buffer. Cells were divided into two aliquots and 2.5 µl of 2 mM CCCP (diluted in DMSO, final concentration was 50 µM) was added. Alternatively, DMSO was added as a control and samples were incubated at room temperature for 10 min. After confirming that the cells stopped swimming completely in CCCP-containing samples under dark-field microscopy, 100 µl of MLM buffer containing 40 µM BMOE was added into each sample (final concentration of 20 µM BMOE) and incubated at room temperature for 1 h in the dark. After the reaction, each sample was centrifuged and washed with 500 µl of Wash buffer. After observing the swimming behavior of the cells, each sample was centrifuged, resuspended in 20 µl of SDS loading buffer with 2-mercaptoethanol and boiled at 100°C for 5 min.

Results

Combinations of FlgI and MotB cysteine mutants used for cross-linking experiments

When we started this project there was very little structural information for FlgI and MotB proteins, so we constructed and analysed a series of Cys-substituted FlgI and MotB mutants (*14, 31*; summarized in Fig. 1). Based on the data, we first surveyed the 32 FlgI Cys mutants and the 13 MotB mutants to select appropriate mutants for investigating possible interaction between FlgI and MotB. We selected mutants based on the following three criteria: (i) the mutant protein is stable; (ii) the mutation does not impair motility of the cells and (iii) the mutation site is expected to be surface exposed as predicted by thiol-specific modification experiments. According to these criteria we chose four FlgI mutants, FlgI G11C, G161C, Y191C, S211C and three MotB mutants, MotB D198C, S248C and A278C.

Disulphide cross-linking between FlgI and MotB cysteine mutants

A FlgI Cys mutant (pYZ301 derivatives) and a wild-type MotA/MotB Cys mutant (pJN726 derivatives) were co-expressed in the *flgI motAmotB* triple deletion strain YZ12-1. We tested swarming motility of cells co-expressing 12 FlgI/MotB Cys mutant combinations in soft-agar plates and those strains showed almost the same motility as the wild-type FlgI/MotB co-expressing strain; hence Cys mutations did not affect cell motility (data not shown). Next we performed immunoblotting analyses using anti-FlgI or MotB antibodies to detect cross-linked products. Without oxidant, FlgI mutants exhibited a monomer band and various cross-linked products probably including a predicted dimer (Fig. 2, left-half of upper panel),

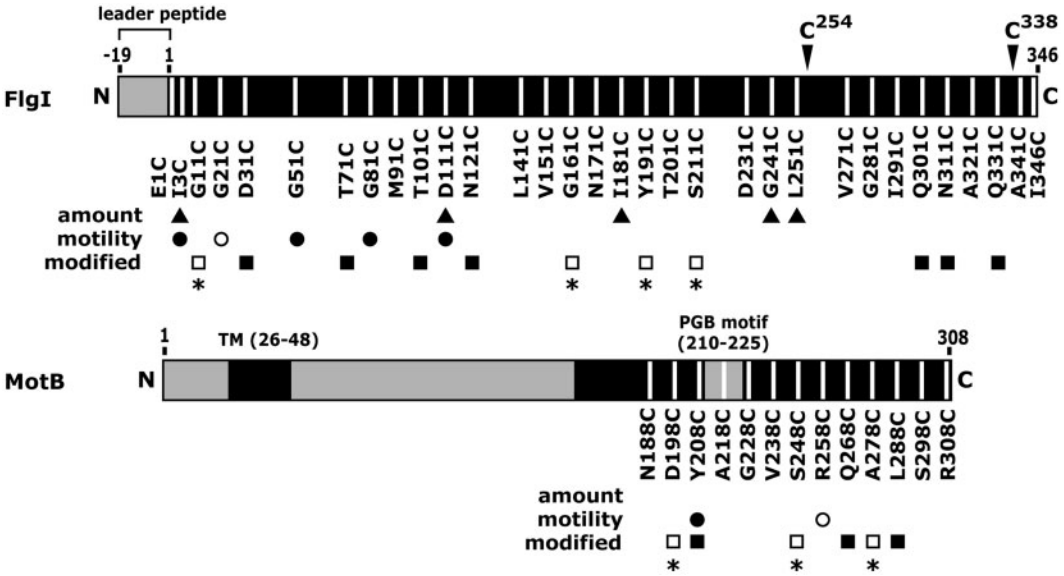

Fig. 1 Characterization of the FlgI and MotB Cys mutants. Profiles of the FlgI (*14*) and MotB (*31*) Cys mutants that were analysed in previous studies are summarized. Amount, the residues for which the protein amount was decreased when substituted with Cys (filled triangle); motility, the residues that caused decreased (filled circle) or completely disrupted (open circle) motility of the cells; modified, the residues that were well- (open square) or moderately- (closed square) labelled by the thiol-specific reagent mPEG-maleimide. Asterisks indicate the mutants that were chosen for combinatorial expression of FlgI and MotB mutants in this work.

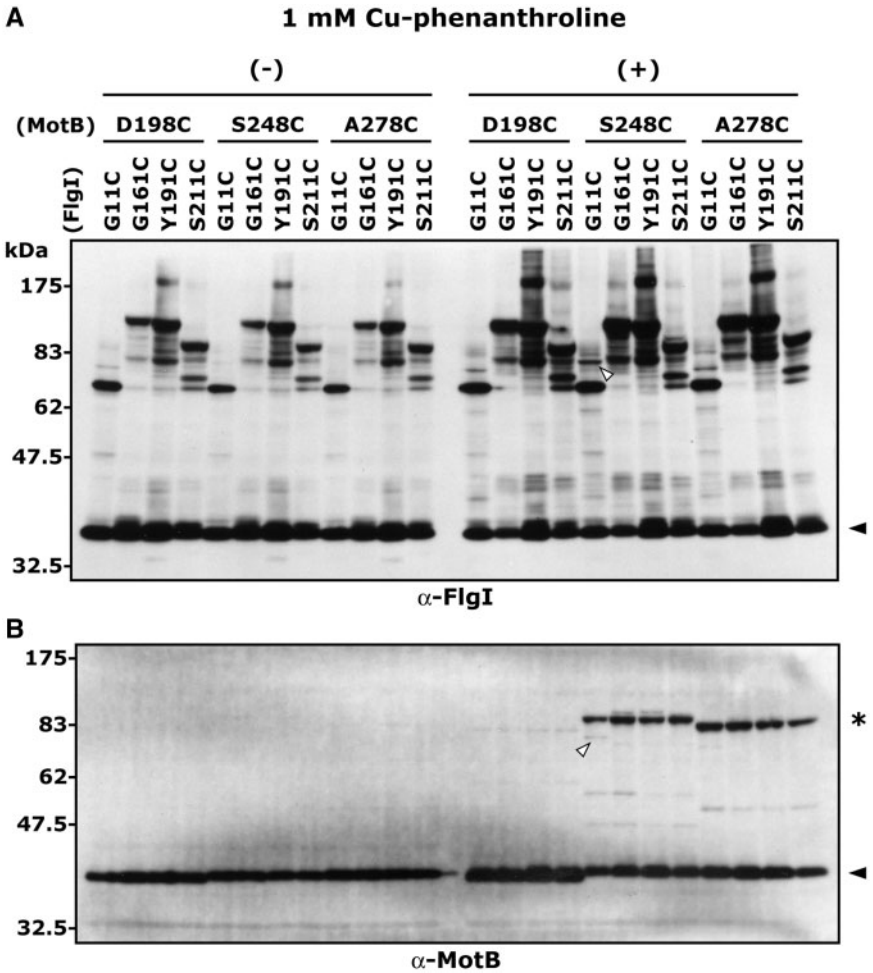

Fig. 2 ***In vivo*** **disulphide cross-linking of cells co-expressing the FlgI and MotB Cys variants by the oxidant Cu-phenanthroline**. The FlgI (A) and the MotB proteins (B) from YZ12-1 (Δ*flgI* Δ*motAB*::*cat*) cells harboring pYZ301 (FlgI) and pJN726 (wild-type MotA/MotB) derivatives possessing Cys mutations were detected by immunoblotting using anti-FlgI and anti-MotB antibodies, respectively. Expression of the MotB proteins was induced with 0.04% L-arabinose. Cells were harvested, washed and incubated with [right-half, (+)] or without [left-half, (−)] 1 mM Cu-phenanthroline at room temperature for 30 min. All samples were prepared without 2-mercaptoethanol. The closed arrowheads on the right side indicate the monomeric forms of FlgI (36 kDa) or MotB (34 kDa); the asterisk indicates the predicted dimer form of MotB; open arrowheads indicate the predicted cross-linked products between the FlgI G11C and MotB S248C mutants.

on the other hand, MotB mutants exhibited only the monomer band (Fig. 2, left-half of lower panel). When treated with the oxidant Cu-phenanthroline, FlgI mutants displayed increased band intensities for almost all of the cross-linked products, and MotB mutants generated a predicted homodimer band (Fig. 2, right-halves of each panel, asterisk). We found a specific band (I-B band) that was detected by both anti-FlgI and anti-MotB antibodies only from the combination of FlgI G11C with MotB S248C, but not with MotB D198C and A278C, although the intensity of the cross-linked band was not strong (Fig. 2, open arrowhead). This specific band seemed to be a cross-linked product between the FlgI and MotB Cys mutants. The predicted FlgI/MotB cross-linked band was not detected when the wild-type protein was co-expressed with the Cys substituted accompanying protein even in the presence of Cu-phenanthroline (Fig. 3A). The predicted I-B bands detected by both anti-FlgI and anti-MotB antibodies appeared to be the same size (Fig. 3B, open arrowhead). The estimated molecular weights of mature-FlgI and MotB are 36 and 34 kDa, respectively, thus, the estimated mass of the I-B heterodimer is 70 kDa. The migration speed of the cross-linked dimers in a gel is retarded by the effect of the branched structure as observed before (*14*). From these results we concluded that the specific band detected in the combination of FlgI G11C/MotB S248C was derived from a disulphide cross-linked product between FlgI and MotB Cys mutant proteins.

Cysteine scanning of residues around FlgI Gly^{11} and MotB Ser^{248}

Disulphide cross-linking between FlgI G11C and MotB S248C suggests that the Gly^{11} residue of FlgI is close to the Ser^{248} residue of MotB. To assess the spatial arrangement around these two residues we performed Cys scanning mutagenesis in these regions of the proteins. We introduced single Cys replacements in FlgI from Thr^{7}–Asn^{15} and in MotB from Arg^{246}–Arg^{250}, respectively. First, we co-expressed the constructed Cys mutants with the wild-type

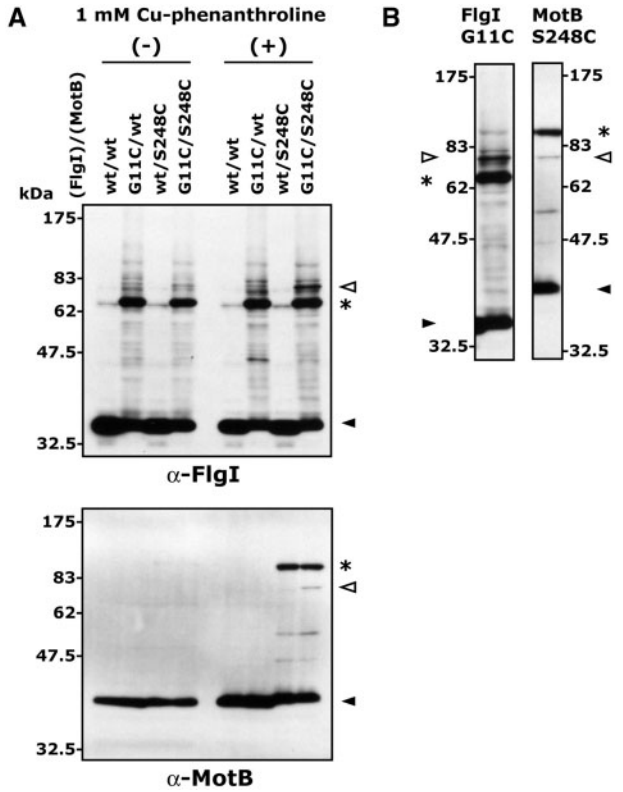

Fig. 3 Detailed analysis of the FlgI G11C/MotB S248C co-expressing strain. (A) FlgI-MotB disulphide specific cross-linked band. FlgI G11C (pYZ301 derivative) or wild-type MotA/MotB S248C (pJN726 derivative) was co-expressed with the wild-type MotA/MotB (pJN726) or FlgI (pYZ301), respectively, in the YZ12-1 (Δ*flgI* Δ*motAB*::*cat*) strain. Each combinatorial strain was treated with [right-half, (+)] or without [left-half, (-)] 1 mM Cu-phenanthroline as in Fig. 2, and the FlgI protein (upper panel) or the MotB protein (lower panel) was detected by immunoblotting with the corresponding antibodies. Only when the FlgI and MotB Cys mutants were co-expressed was a specific band detected depending on the oxidant treatment (open arrowheads). The closed arrowheads indicate the monomeric forms of FlgI (36 kDa) or MotB (34 kDa); the asterisks indicate the predicted dimer form of FlgI or MotB. (B) Comparison of the size of the specific disulphide cross-linked band. The rightmost lane of each panel in (A) was excised, adjusted for the molecular marker size and aligned side by side. The two predicted cross-linked bands between FlgI G11C and MotB S248C detected with anti-FlgI and anti-MotB antibodies, respectively, seemed to be identical in size (open arrowheads).

accompanying proteins in YZ12-1 to investigate the characteristics of each Cys mutant protein. Cells expressing these Cys mutant proteins exhibited almost normal motility on soft-agar plates except for FlgI N15C, whose motility was completely abolished (data not shown). MotB Asp^{249}, for which Val substitution affects motility of *Salmonella* in semi-solid agar plates (*40*), did not affect motility in *E. coli*. Immunoblotting analysis showed that expression of all of the Cys mutant proteins was almost the same (data not shown). Next, we co-expressed FlgI Cys mutants with MotB S248C, or co-expressed FlgI G11C with MotB Cys mutants in strain YZ12-1 and assessed the cross-linking efficiencies between FlgI and the MotB Cys mutants (Fig. 4). As described above, FlgI N15C did not confer motility. In addition, the motility of the strain carrying FlgI V9C was slightly decreased, but the other Cys mutants did not cause a significant change in motility when co-expressed with MotB S248C (Fig. 4A, left panel). The newly generated MotB Cys mutants conferred the same motility phenotypes when co-expressed with FlgI G11C as with the wild-type FlgI (Fig. 4A, right panel). We performed immunoblotting analysis after the cells were treated with Cu-phenanthroline (Fig. 4B). FlgI S8C displayed the same band intensity of the predicted I-B band as FlgI G11C, and the band intensities of FlgI Q10C and R13C were slightly decreased (Fig. 4B, open arrowhead in left panel). In the MotB mutants, all five MotB mutants displayed clear I-B bands in addition to the dimer bands (asterisk), and the I-B bands formed by MotB R250C were significantly stronger than the others (Fig. 4B, open arrowhead in right panel). These results may suggest that Arg^{250} of MotB can approach spatially closer to Gly^{11} of FlgI or can stay temporally longer near Gly^{11} of FlgI than other residues.

Cross-linking methods that do not impair cell motility

We detected disulphide cross-linking between the FlgI and MotB Cys mutants; however, the Cu-phenanthroline treatment made the bacterial cells non-motile even when wild-type cells were treated. We wanted to cross-link proteins under conditions that did not affect cell motility. Therefore, we tried other oxidants, $CuCl_2$ and 5,5′-dithiobis-2-nitrobenzoic acid (DTNB), but no cross-linked products between FlgI and MotB were detected. Next, we used various cross-linkers including three bismaleimide cross-linkers, bis(maleimido)hexane (BMH), 1,4-bis(maleimido)butane (BMB) and bis(maleimido) ethane (BMOE), which have two maleimide-groups in both heads and bind to thiol-groups specifically and irreversibly. Each has a different arm length: BMH, 13.0 Å; BMB, 10.9 Å; BMOE, 8.0 Å. We treated the FlgI G11C/MotB R250C co-expressing cells with several concentrations of these cross-linkers, and detected predicted I-B bands at certain concentrations of each cross-linker (Fig. 5, open arrowhead). The optimal concentrations of the cross-linkers seemed to depend on the arm length. It appeared that the excess cross-linkers bound to both thiol-groups of FlgI and MotB Cys mutants and consequently cross-linking between FlgI and MotB was inhibited. Because longer cross-linker (hence having larger molecular mass) is expected to have more difficulty accessing the target site than the shorter one, it is thought to be reasonable that the optimal concentration of longer cross-linkers was higher. Even after the cross-linking treatment, the cells were still motile when observed by dark-field microscopy, although their swimming fraction was slightly decreased (data not shown). We also examined other cross-linkers, including 1,4-di-[3′-(2′-pyridyldithio) propionamido] butane (DPDPB), which is a reversible thiol-reactive cross-linker and tris-[2-maleimidoethyl]amine (TMEA), which is a trifunctional maleimide cross-linker. The former exhibited a very low cross-linking efficiency and the latter gave a complicated pattern of cross-linking products (data not shown).

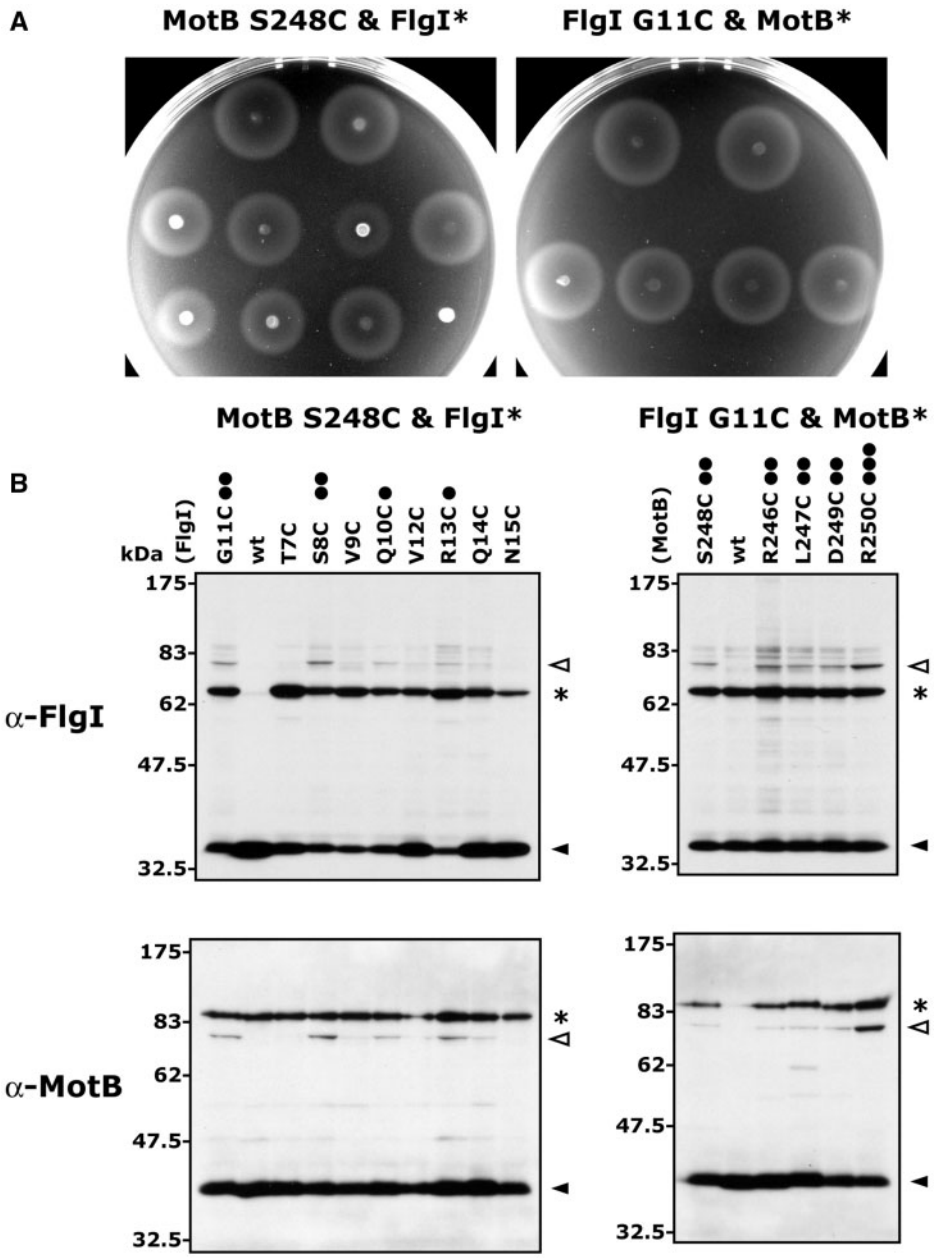

Fig. 4 Cysteine scanning experiment around the FlgI Gly[11] and MotB Ser[248] residues. (A) Motility of the FlgI and MotB Cys mutant co-expressing cells. Left panel, wild-type MotA/MotB S248C (pJN726 derivative) and a series of FlgI Cys variants (pYZ301 derivatives possessing single Cys mutations) were co-expressed in the YZ12-1 (Δ*flgI* Δ*motAB*::*cat*) strain; right panel, FlgI G11C and a series of MotB Cys variants were co-expressed. A drop (2 µl) of overnight culture was inoculated on 0.27% soft-agar T broth plates and incubated at 30°C for 6 h. (B) Cu-phenanthroline treatment. The FlgI and MotB Cys mutant co-expressing strains were treated with 1 mM Cu-phenanthroline as in Fig. 2 and each protein was immunodetected with anti-FlgI (upper panel) or anti-MotB (lower panel) antibodies, respectively. The closed arrowheads indicate the monomeric forms of FlgI (36 kDa) or MotB (34 kDa); the asterisks indicate the predicted dimer form; open arrowheads indicate the predicted cross-linked products between the FlgI and MotB Cys mutants. The closed circles on the upper side of the panels show the relative cross-linking efficiencies by the number of closed circles.

Since BMOE had a lower optimal concentration for cross-linking than the others, we chose 20 µM BMOE treatment for FlgI/MotB cross-linking, a concentration that did not impair cell motility, for the following experiments. It should be noted that when we co-expressed FlgI G11C and MotB R250C in a strain in which no flagellar protein was expressed (*flhDC* deletion strain RP3098) as a control experiment, we still detected a predicted cross-linked band between the mature-form of FlgI and MotB in this strain (see below). This suggests that the FlgI proteins that did not form the P ring in the periplasmic space can form a disulphide-bridge with MotB proteins located in membrane.

Change of the cross-linking efficiency depending on proton motive force

Fluorescent recovery after photobleaching experiments using GFP-fused stator proteins in *E. coli* have revealed that the stator complexes incorporated into

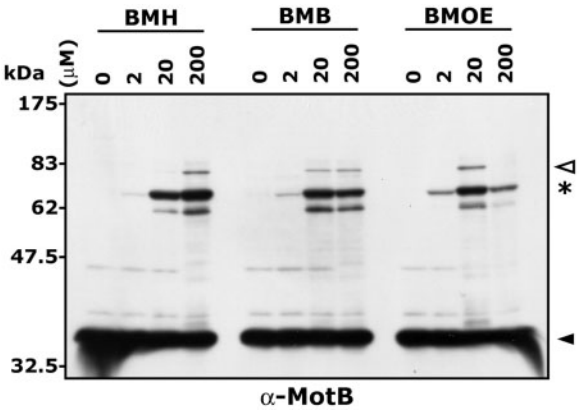

Fig. 5 Cross-linking between FlgI G11C/MotB R250C using bismaleimide cross-linkers. YZ12-1 (Δ*flgI* Δ*motAB*::*cat*) cells harboring pYZ301 FlgI G11C and pJN726 MotB R250C were treated with three bismaleimide cross-linkers, BMH, BMB and BMOE. Expression of MotB proteins was induced with 0.04% L-arabinose. Cells were harvested, washed and incubated with each cross-linker at the indicated concentrations at room temperature for 1 h. All samples were treated with 2-mercaptoethanol and the MotB protein was detected by immunoblotting using anti-MotB antibodies. The closed arrowheads indicate the monomeric forms of MotB (34 kDa); the asterisk indicates the predicted dimer form; open arrowheads indicate the predicted cross-linked products between FlgI G11C/MotB R250C.

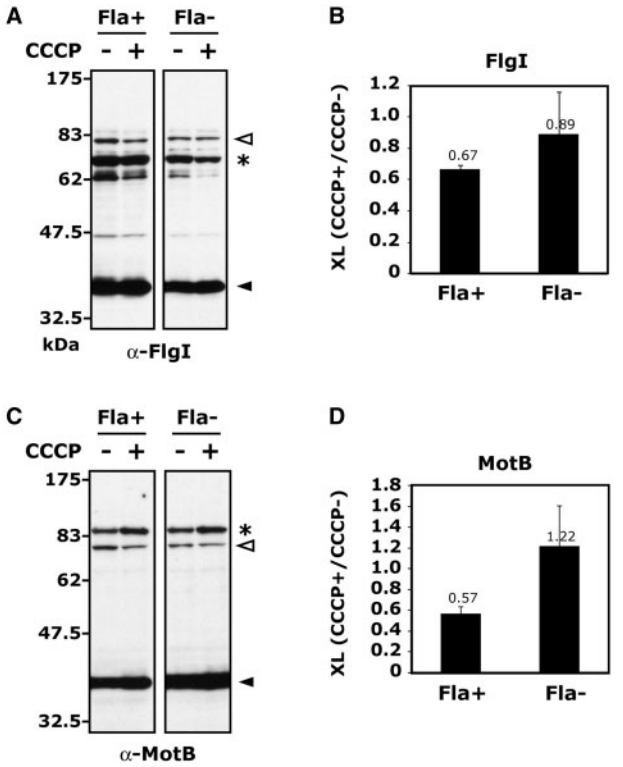

Fig. 6 Change of cross-linking efficiency caused by CCCP. Cells of the flagellated strain YZ12-1 (Δ*flgI* Δ*motAB*::*cat*, Fla^+) or the non-flagellated strain RP3098 (Δ(*flhD-flhA*)*4*, Fla^-) harboring pYZ301 FlgI G11C and pJN726 MotB R250C were harvested, washed and incubated with or without 50 μM CCCP at room temperature for 10 min. and each sample was subsequently treated with 20 μM BMOE for 1 h. All samples were treated with 2-mercaptoethanol and the FlgI and MotB proteins were detected by immunoblotting using anti-FlgI (A) or anti-MotB (C) antibodies. The closed arrowheads indicate the monomeric forms of FlgI (36 kDa) or MotB (34 kDa); the asterisks indicate the predicted homodimer; open arrowheads indicate the predicted cross-linked products between FlgI G11C/MotB R250C. (B and D) The changing rate of cross-linking efficiency was calculated by dividing the FlgI/MotB cross-linking band intensity in the presence of CCCP by that in the absence of CCCP. They were calculated for the FlgI protein (B) and the MotB protein (D), respectively. Each experiment was repeated five times independently and average values are presented. Error bars indicate standard deviations.

the motor exchanged frequently with those present in the membrane pool around the motor (*32*). In another study in *Vibrio alginolyticus*, which has a Na^+-driven flagellar motor, fluorescence observation experiments using GFP-PomB indicated that the stator complexes PomA/PomB (homolog of MotA/MotB) are immediately dissociated from the flagellar motor in the absence of the coupling ion Na^+, i.e. in the absence of a Na^+ gradient (*33*). In the proton-driven motor of *E. coli*, it has been reported that individual stator complexes are inactivated at low proton motive force and speculated that the mechanism of inactivation may involve the dissociation of the MotA and/or MotB components (*41*). Thus, the MotA/MotB stator complexes are expected to dissociate from the flagellar motor when treated with carbonyl cyanide *m*-chlorophenylhydrazone (CCCP), a protonophore that abolishes H^+ gradients. Since we established cross-linking conditions in which cell motility is not affected, we were able to investigate the effect of CCCP on FlgI-MotB cross-linking in functional motors. First, we confirmed that *E. coli* cells completely lost swimming motility in the presence of 50 μM CCCP. Next we observed localization of GFP-MotB in the presence of CCCP using fluorescent microscopy with strain JPA750 (gift from Judith Armitage), which expresses GFP-MotB protein from the chromosome instead of the native MotB. The number of fluorescent foci significantly decreased in the presence of CCCP, indicating that the CCCP treatment disassembled the stator complexes around the flagellar motor (data not shown). Then we performed a BMOE cross-linking experiment using YZ12-1 cells co-expressing FlgI G11C and MotB R250C in the presence of CCCP. The ratio of the I-B band intensity in the presence of CCCP to that in the absence of CCCP was calculated as a changing rate of cross-linking efficiency (Fig. 6). The I-B band intensity in both FlgI and MotB blots was significantly reduced when cells were treated with CCCP prior to the cross-linking reaction (open triangle in Fla^+ lanes). On the other hand, when the same experiment was performed in the non-flagellated *flhDC* deletion background, effect of CCCP on the I-B band intensity was smaller; similar bands were detected in both the FlgI and MotB blots. This difference is shown more clearly in the changing rate of cross-linking efficiencies caused by CCCP treatment, obtained from five repetitions of the experiment (Fig. 6B and D), which is lower in YZ12-1 cells (flagellated strain) than in RP3098 cells (non-flagellated strain). These results imply that the interaction between FlgI and MotB is facilitated in the presence of proton motive force in flagellated cells, probably because the stators can be assembled around a functional flagellar motor.

Discussion

In *Borrelia burgdorferi*, spirochetes that have periplasmic flagella, the *in situ* image from cryo-electron tomography showed a structure that appears to bridge the stator and the rotor (*42*). In *Vibrio* species, MotX/MotY, which are components of the T ring located on the periplasmic side of the P ring, have been reported to be involved in stator assembly (*38*). However, *E. coli* does not have MotX and MotY. It has been shown that the C-terminal region of MotB plays an important role in targeting and stable anchoring of the stator complex to putative stator-binding sites of the motor (*37*). However, it remains unknown where the stator-binding sites are in the motor. In this study, we assessed disulphide cross-linking between FlgI and MotB Cys mutants. We showed that several FlgI and MotB Cys mutants generated a specific cross-linked product (Fig. 4). We suggest that the P ring provides binding sites for assembly of the stator into a motor.

Cross-linking efficiency was not very high in the experiment. We think this low efficiency is not surprising and reasonable because only a small fraction of the stator complexes can assemble around the rotor or many FlgI molecules are not always used for the ring structure. Furthermore, it has been shown that over-expression of the hook protein FlgE suppresses the *E. coli flgA*, *flgH* and *flgI* mutants to significant degree (*43*), indicating that even in the absence of P ring partial incorporation of stator into a motor can be achieved. This may explain the low efficiency of cross-link and imply that MotB–FlgI interaction is not essential, but since this suppression did not cause full restoration of motility we assume that MotB–FlgI interaction shown here may be required for efficient incorporation or stably anchoring around the rotor to become fully functioning motor. Recent findings have revealed that the stator showed dynamic assembly/dissociation around the motor (*32–34*), suggesting the presence of efficient motor-recognition mechanisms and consistent with our idea.

We present a predicted spatial relationship between the stator and the bearing from the evidence of this study and our structural data of MotB (*26*) (Fig. 7). Because structural information for the FlgI protein is not available, it is difficult to discuss the position of the FlgI Gly^{11} residue or other residues that were confirmed to cross-link with MotB in this study. We previously found that Gly^{11} of FlgI seems to be surface exposed in a significant fraction of time (*14*). FlgI variants with Cys substitution for Ser^{8}, Gln^{10} and Arg^{13} were able to cross-link with MotB (Fig. 4), indicating that these Cys residues are also surface exposed. Since these residues are located in the highly conserved N-terminal region of FlgI (*14*), therefore, we propose that the highly conserved, surface-exposed N-terminal domain of FlgI is a binding site for MotB. The crystal structures of the C-terminal periplasmic region of MotB of *H. pylori* (*25*) or *S. enterica* (*26*) have been already solved. We mapped the residues that cross-linked with FlgI in this study on the dimer structure of the periplasmic region of *Salmonella* MotB

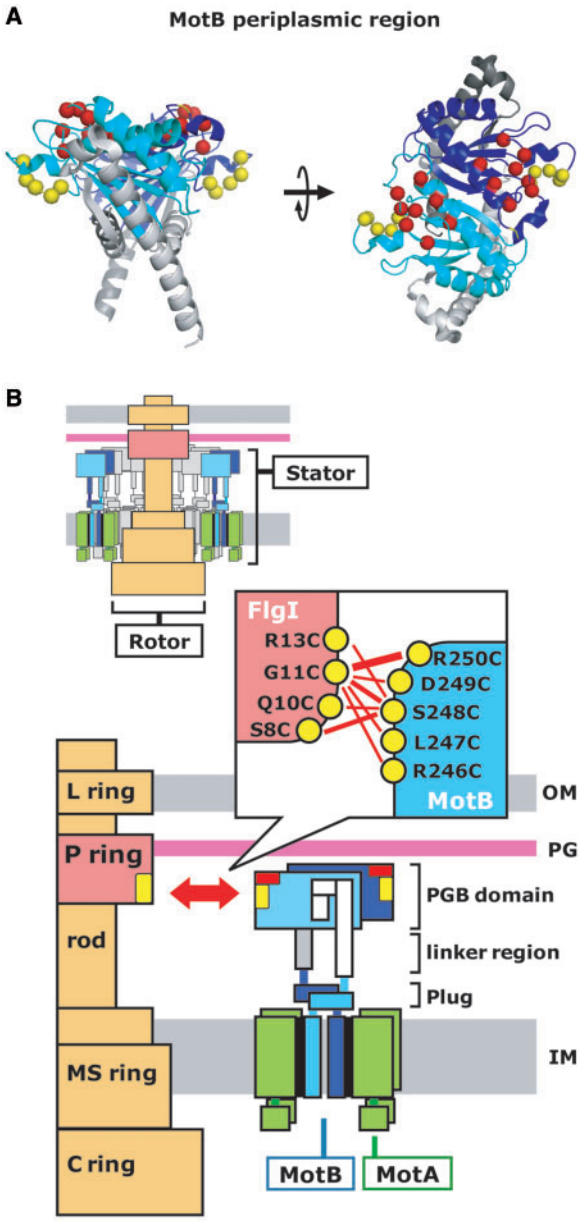

Fig. 7 Schematic diagram of the structures of FlgI and MotB in the functional motor. (A) The crystal structure of the dimer form of the C-terminal periplasmic region of *Salmonella* MotB (2ZVY, *26*) is shown. Left, side view; right, top view. The PGB domain (146–264 in *Salmonella*) of one monomer is coloured cyan and the other one is coloured blue. The linker region is coloured white or grey. The residues in *E. coli* that cross-linked with FlgI Cys mutants in this work were mapped and are shown as yellow spheres. The predicted residues contributing to PG binding proposed by Kojima *et al.* (*26*) are shown as red spheres. (B) Schematic diagrams of the flagellar motor (upper) and the possible interaction between the P ring (FlgI) and the stator (MotB) proposed by this work (lower). The residue-pairs demonstrated to cross-link in this work are shown in the box. Coloured regions in MotB are described as (A). OM, outer membrane; PG, peptidoglycan; IM, inner membrane.

(Fig. 7A, yellow spheres). These residues were positioned on the protruding loop in the PGB domain, hence it is not likely to disturb its ternary structure even if this loop region contacts to the P ring. Each PGB domain in the MotB dimer is located in anti-parallel orientation in the crystal structure. Therefore, FlgI-contacting loops would be positioned

in each end of MotB dimer (Fig. 7A). From this assumption only one loop in the MotB dimer is predicted to contact FlgI when the stator is incorporated into the motor.

Conformational changes of the stator have been proposed to occur when the stator is incorporated into the motor and starts to generate torque. The MotB 'Plug' region, which is located just after the TM region of MotB, has been proposed to block proton leakage when the MotA/MotB stator is in the membrane pool, and to be in the open state when the stator is incorporated into the motor (*44*, *45*). Based on the crystal structure of the MotB periplasmic region, the linker region between the PGB domain and the Plug region in MotB has been proposed to extend to allow the PGB domain to reach the PG layer when the stator is incorporated into the motor (*26*). The Plug region should be open and the stator should be anchored to the PG layer via the PGB domain before proton flow and torque generation occurs. So it might be reasonable that the stator–motor interaction in the periplasmic space would be an initial event that triggers the sequence of stator conformational changes.

Acknowledgements

We thank Toshiharu Yakushi and Ikuro Kawagishi for invaluable discussions and Yuki Sudo and Kingo Takiguchi for helpful advice.

Funding

Grants-in-aid for scientific research from the Ministry of Education, Science, and Culture of Japan (to M.H.), partial; the Japan Science and Technology Corporation (to M.H. and S.K.); the Japan Society for the Promotion of Science (to Y.H.).

Conflict of interest

None declared.

References

1. Macnab, R.M. (2003) How bacteria assemble flagella. *Annu. Rev. Microbiol.* **57**, 77–100
2. Blair, D.F. and Berg, H.C. (1990) The MotA protein of *E. coli* is a proton-conducting component of the flagellar motor. *Cell* **60**, 439–449
3. Dean, G.E., Macnab, R.M., Stader, J., Matsumura, P., and Burks, C. (1984) Gene sequence and predicted amino acid sequence of the *motA* protein, a membrane-associated protein required for flagellar rotation in *Escherichia coli*. *J. Bacteriol.* **159**, 991–999
4. Stader, J., Matsumura, P., Vacante, D., Dean, G.E., and Macnab, R.M. (1986) Nucleotide sequence of the *Escherichia coli motB* gene and site-limited incorporation of its product into the cytoplasmic membrane. *J. Bacteriol.* **166**, 244–252
5. Stolz, B. and Berg, H.C. (1991) Evidence for interactions between MotA and MotB, torque-generating elements of the flagellar motor of *Escherichia coli*. *J. Bacteriol.* **173**, 7033–7037
6. Akiba, T., Yoshimura, H., and Namba, K. (1991) Monolayer crystallization of flagellar L-P rings by sequential addition and depletion of lipid. *Science* **252**, 1544–1546
7. Jones, C.J., Macnab, R.M., Okino, H., and Aizawa, S. (1990) Stoichiometric analysis of the flagellar hook-(basal-body) complex of *Salmonella typhimurium*. *J. Mol. Biol.* **212**, 377–387
8. Sosinsky, G.E., Francis, N.R., DeRosier, D.J., Wall, J.S., Simon, M.N., and Hainfeld, J. (1992) Mass determination and estimation of subunit stoichiometry of the bacterial hook-basal body flagellar complex of *Salmonella typhimurium* by scanning transmission electron microscopy. *Proc. Natl Acad. Sci. USA* **89**, 4801–4805
9. Homma, M., Komeda, Y., Iino, T., and Macnab, R.M. (1987) The *flaFIX* gene product of *Salmonella typhimurium* is a flagellar basal body component with a signal peptide for export. *J. Bacteriol.* **169**, 1493–1498
10. Kubori, T., Shimamoto, N., Yamaguchi, S., Namba, K., and Aizawa, S. (1992) Morphological pathway of flagellar assembly in *Salmonella typhimurium*. *J. Mol. Biol.* **226**, 433–446
11. Nambu, T. and Kutsukake, K. (2000) The S*almonella* FlgA protein, a putativeve periplasmic chaperone essential for flagellar P ring formation. *Microbiology* **146**, 1171–1178
12. Dailey, F.E. and Berg, H.C. (1993) Mutants in disulfide bond formation that disrupt flagellar assembly in *Escherichia coli*. *Proc. Natl Acad. Sci. USA* **90**, 1043–1047
13. Hizukuri, Y., Yakushi, T., Kawagishi, I., and Homma, M. (2006) Role of the intramolecular disulfide bond in FlgI, the flagellar P-ring component of *Escherichia coli*. *J. Bacteriol.* **188**, 4190–4197
14. Hizukuri, Y., Kojima, S., Yakushi, T., Kawagishi, I., and Homma, M. (2008) Systematic Cys mutagenesis of FlgI, the flagellar P-ring component of *Escherichia coli*. *Microbiology* **154**, 810–817
15. Zhou, J., Fazzio, R.T., and Blair, D.F. (1995) Membrane topology of the MotA protein of *Escherichia coli*. *J. Mol. Biol.* **251**, 237–242
16. Chun, S.Y. and Parkinson, J.S. (1988) Bacterial motility: membrane topology of the *Escherichia coli* MotB protein. *Science* **239**, 276–278
17. Braun, T.F., Al-Mawsawi, L.Q., Kojima, S., and Blair, D.F. (2004) Arrangement of core membrane segments in the MotA/MotB proton-channel complex of *Escherichia coli*. *Biochemistry* **43**, 35–45
18. Kojima, S. and Blair, D.F. (2004) Solubilization and purification of the MotA/MotB complex of *Escherichia coli*. *Biochemistry* **43**, 26–34
19. Sato, K. and Homma, M. (2000) Functional reconstitution of the Na^+-driven polar flagellar motor component of *Vibrio alginolyticus*. *J. Biol. Chem.* **275**, 5718–5722
20. Yorimitsu, T., Kojima, M., Yakushi, T., and Homma, M. (2004) Multimeric structure of the PomA/PomB channel complex in the Na^+-driven flagellar motor of *Vibrio alginolyticus*. *J. Biochem.* **135**, 43–51
21. Reid, S.W., Leake, M.C., Chandler, J.H., Lo, C.J., Armitage, J.P., and Berry, R.M. (2006) The maximum number of torque-generating units in the flagellar motor of *Escherichia coli* is at least 11. *Proc. Natl Acad. Sci. USA* **103**, 8066–8071
22. Blair, D.F. (2003) Flagellar movement driven by proton translocation. *FEBS Lett.* **545**, 86–95
23. De Mot, R. and Vanderleyden, J. (1994) The C-terminal sequence conservation between OmpA-related outer membrane proteins and MotB suggests a common function in both gram-positive and gram-negative bacteria, possibly in the interaction of these domains with peptidoglycan. *Mol. Microbiol.* **12**, 333–334
24. Koebnik, R. (1995) Proposal for a peptidoglycan-associating alpha-helical motif in the C-terminal regions

of some bacterial cell-surface proteins. *Mol. Microbiol.* **16**, 1269–1270
25. Roujeinikova, A. (2008) Crystal structure of the cell wall anchor domain of MotB, a stator component of the bacterial flagellar motor: implications for peptidoglycan recognition. *Proc. Natl Acad. Sci. USA* **105**, 10348–10353
26. Kojima, S., Imada, K., Sakuma, M., Sudo, Y., Kojima, C., Minamino, T., Homma, M., and Namba, K. (2009) Stator assembly and activation mechanism of the flagellar motor by the periplasmic region of MotB. *Mol. Microbiol.* **73**, 710–718
27. Bouveret, E., Benedetti, H., Rigal, A., Loret, E., and Lazdunski, C. (1999) In vitro characterization of peptidoglycan-associated lipoprotein (PAL)-peptidoglycan and PAL-TolB interactions. *J. Bacteriol.* **181**, 6306–6311
28. Lazzaroni, J.C. and Portalier, R. (1992) The *excC* gene of *Escherichia coli* K-12 required for cell envelope integrity encodes the peptidoglycan-associated lipoprotein (PAL). *Mol. Microbiol.* **6**, 735–742
29. Leduc, M., Ishidate, K., Shakibai, N., and Rothfield, L. (1992) Interactions of *Escherichia coli* membrane lipoproteins with the murein sacculus. *J. Bacteriol.* **174**, 7982–7988
30. Mizuno, T. (1979) A novel peptidoglycan-associated lipoprotein found in the cell envelope of *Pseudomonas aeruginosa* and *Escherichia coli*. *J. Biochem.* **86**, 991–1000
31. Hizukuri, Y., Morton, J.F., Yakushi, T., Kojima, S., and Homma, M. (2009) The peptidoglycan-binding (PGB) domain of the *Escherichia coli* Pal protein can also function as the PGB domain in *E. coli* flagellar motor protein MotB. *J. Biochem.* **146**, 219–229
32. Leake, M.C., Chandler, J.H., Wadhams, G.H., Bai, F., Berry, R.M., and Armitage, J.P. (2006) Stoichiometry and turnover in single, functioning membrane protein complexes. *Nature* **443**, 355–358
33. Fukuoka, H., Wada, T., Kojima, S., Ishijima, A., and Homma, M. (2009) Sodium-dependent dynamic assembly of membrane complexes in sodium-driven flagellar motors. *Mol. Microbiol.* **71**, 825–835
34. Paulick, A., Koerdt, A., Lassak, J., Huntley, S., Wilms, I., Narberhaus, F., and Thormann, K.M. (2009) Two different stator systems drive a single polar flagellum in *Shewanella oneidensis* MR-1. *Mol. Microbiol.* **71**, 836–850
35. Yakushi, T., Hattori, N., and Homma, M. (2005) Deletion analysis of the carboxyl-terminal region of the PomB component of the *Vibrio alginolyticus* polar flagellar motor. *J. Bacteriol.* **187**, 778–784
36. Fukuoka, H., Yakushi, T., Kusumoto, A., and Homma, M. (2005) Assembly of motor proteins, PomA and PomB, in the Na^+-driven stator of the flagellar motor. *J. Mol. Biol.* **351**, 707–717
37. Kojima, S., Furukawa, Y., Matsunami, H., Minamino, T., and Namba, K. (2008) Characterization of the periplasmic domain of MotB and implications for its role in the stator assembly of the bacterial flagellar motor. *J. Bacteriol.* **190**, 3314–3322
38. Terashima, H., Fukuoka, H., Yakushi, T., Kojima, S., and Homma, M. (2006) The *Vibrio* motor proteins, MotX and MotY, are associated with the basal body of Na^+-driven flagella and required for stator formation. *Mol. Microbiol.* **62**, 1170–1180
39. Okabe, M., Yakushi, T., and Homma, M. (2005) Interactions of MotX with MotY and with the PomA/PomB sodium ion channel complex of the *Vibrio alginolyticus* polar flagellum. *J. Biol. Chem.* **280**, 25659–25664
40. Togashi, F., Yamaguchi, S., Kihara, M., Aizawa, S.I., and Macnab, R.M. (1997) An extreme clockwise switch bias mutation in *fliG* of *Salmonella typhimurium* and its suppression by slow-motile mutations in *motA* and *motB*. *J. Bacteriol.* **179**, 2994–3003
41. Fung, D.C. and Berg, H.C. (1995) Powering the flagellar motor of *Escherichia coli* with an external voltage source. *Nature* **375**, 809–812
42. Kudryashev, M., Cyrklaff, M., Wallich, R., Baumeister, W., and Frischknecht, F. (2009) Distinct *in situ* structures of the *Borrelia* flagellar motor. *J. Struct. Biol.* **69**, 54–61
43. Ohnishi, K., Homma, M., Kutsukake, K., and Iino, T. (1987) Formation of flagella lacking outer rings by *flaM*, *flaU*, and *flaY* mutants of *Escherichia coli*. *J. Bacteriol.* **169**, 1485–1488
44. Hosking, E.R., Vogt, C., Bakker, E.P., and Manson, M.D. (2006) The *Escherichia coli* MotAB proton channel unplugged. *J. Mol. Biol.* **364**, 921–937
45. Morimoto, Y.V., Che, Y.S., Minamino, T., and Namba, K. (2010) Proton-conductivity assay of plugged and unplugged MotA/B proton channel by cytoplasmic pHluorin expressed in *Salmonella*. *FEBS Lett.* **584**, 1268–1272
46. Parkinson, J.S. and Houts, S.E. (1982) Isolation and behavior of *Escherichia coli* deletion mutants lacking chemotaxis functions. *J. Bacteriol.* **151**, 106–113
47. Slocum, M.K. and Parkinson, J.S. (1983) Genetics of methyl-accepting chemotaxis proteins in *Escherichia coli*: organization of the tar region. *J. Bacteriol.* **155**, 565–577
48. Guzman, L.M., Belin, D.M., Carson, J., and Beckwith, J. (1995) Tight regulation, modulation, and high-level expression by vectors containing the arabinose P_{BAD} promoter. *J. Bacteriol.* **177**, 4121–4130
49. Bartolome, B., Jubete, Y., Martinez, E., and de la Cruz, F. (1991) Construction and properties of a family of pACYC184-derived cloning vectors compatible with pBR322 and its derivatives. *Gene* **102**, 75–78